# Properties of branched confined polymers

**ARTICLE** *in* THE JOURNAL OF CHEMICAL PHYSICS · MAY 2004

Impact Factor: 2.95 · DOI: 10.1063/1.1687317 · Source: PubMed



**2 AUTHORS:**

Andrzej Sikorski
University of Warsaw
**112** PUBLICATIONS **874** CITATIONS
SEE PROFILE

Piotr Romiszowski
University of Warsaw
**71** PUBLICATIONS **430** CITATIONS
SEE PROFILE

# Properties of branched confined polymers

Andrzej Sikorski and Piotr Romiszowski[a)]
*Department of Chemistry, University of Warsaw, Pasteura 1, 02-093 Warszawa, Poland*

(Received 17 October 2003; accepted 23 January 2004)

A model of star-branched polymer chains confined in a slit formed by two parallel surfaces was studied. The chains were embedded to a simple cubic lattice and consisted of $f=3$ branches of equal length. The macromolecules had the excluded volume and the confining surfaces were impenetrable for polymer segments. No attractive interactions between polymer segments and then between polymer segments and the surfaces were assumed and therefore the system was a thermal. Monte Carlo simulations were carried out employing the sampling algorithm based on chain's local changes of conformation. Lateral diffusion of star-branched chains was studied. Dynamic properties of star-branched chains between the walls with impenetrable rod-like obstacles were also studied and compared to the previous case. The density profiles of polymer segments on the slit were determined. The analysis of contacts between the polymer chain and the surfaces was also carried out. © *2004 American Institute of Physics.* [DOI: 10.1063/1.1687317]

## INTRODUCTION

The problem of the properties of polymeric systems that are observed in a special environment has attracted the attention of numerous researchers in recent years. The modern technology of polymers as well as their applications requires the solution of basic theoretical problems connected with the specific geometrical confinement. Polymeric systems exhibit quite different properties when compared to the melt or solution systems in unrestricted three-dimensional space. The presence of geometrical constraints causes a considerable shrinking of the conformational space of the system.[1] These affect both the static and dynamical properties of chains. The confinement changes the properties of the molecule, which does not behave as a free chain-geometrical obstacles reduce the configuration space. Also the interactions with confining obstacles deform the molecule.[2] The space confinement most frequently used in the literature was a slit which served as a tool for investigations of the properties of linear polymers in thin layers, microstructures, and finally in biosystems.[3–11] Moreover, the cylindrical space confining the molecules was also applied in simulations.[12–16] Some papers were devoted to the static and dynamic properties of a polymer melt in confinement.[17–31] All mentioned works have reported the system anisotropy, which affected the specific properties of the systems.

The great majority of the above-mentioned works are devoted to confined linear polymer chains. The properties of star branched polymers in unrestricted space have recently been studied. The authors have paid attention to both the static and dynamic properties of the systems under consideration. The star-branched molecules appear to be nice stepping-stone model objects for studying the systems in which the topology of the molecule plays an important role.[32,33] The simplest star-branched polymers are the molecules with $f=3$ arms of equal length emanating from a common origin (a branching point). As has been shown, such objects sometimes exhibit properties different from their linear counterparts. The differences are mostly caused by the nonuniform density of stars as well as by the interactions between the arms.

During last two decades simple models of star-branched chains were developed and studied by means of computer simulations.[34–40] It was shown that such simple and naive models can give insight into structure of star-branched chain and to point out the differences in static and dynamic properties when compared with linear chains. In our previous paper we presented the dependence of dimensions of the confined star-branched polymer chain on the distance between the confining impenetrable parallel surfaces.[40] The resulting dependence formed a ''master'' curve, which was valid for all chain lengths. Some dynamic properties of star-branched chains were also studied.[39,40]

In this paper we continue simulation studies on the star-branched polymers. The main goal of this work was to find some universal scaling behavior of the dynamic properties of single confined star-branched chains as well as to collect some information about the structure of the chain compressed in the slit. In order to discuss the problem of the mechanism of motion of star polymers in the confinement we additionally studied the polymer system with a set of impenetrable obstacles introduced into the system.

The organization of the paper is as follows. In the next section we describe the model used in simulations. Then we present the results of the simulations and their explanations. Finally, we present the most important and general features of the system studied.

## THE MODEL AND THE ALGORITHM

We studied a simplified model of star-branched polymers.[34,36] Each model macromolecule consisted of $f=3$ chains (arms) of equal length $n$ emanating from a com-

a)Author to whom all correspondence should be addressed; electronic mail: prom@chem.uw.edu.pl

 

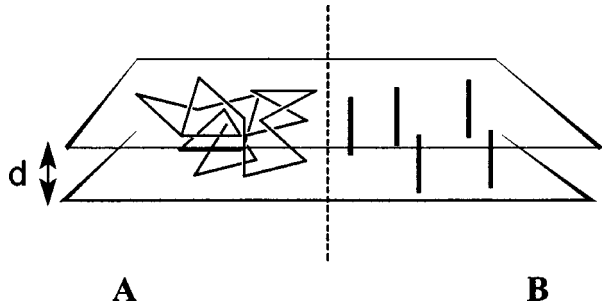


FIG. 1. The scheme of star-branched chain located between two parallel walls without (a) and with rod-like obstacles (b).

mon origin (the branching point). Therefore, the total number of beads in the chain was $N=f(n-1)+1$. The chains were restricted to a simple cubic lattice in order to make the simulations more efficient and in order to made the results comparable to our previous calculations and other results. The polymer beads did not interact by an attractive potential and the excluded volume was the only interaction included into the model. Therefore, the model should reproduce the properties of polymer chains at good solvent conditions. The model star-branched chains were confined to a slit formed by two impenetrable surfaces, which was schematically depicted in Fig. 1(a). No attractive interaction between the surfaces and polymer segments was assumed, hence the influence of the walls was entropic only. We chose the orientation of these surfaces assuming they were parallel to the *xy* plane. The Monte Carlo box had the edge large enough to study the longer chains ($L=200$) in *x* and *y* directions with the periodic boundary conditions.

The properties of model chains were studied by means of the Monte Carlo method. The Metropolis-type algorithm was used to sample the conformational space. A chain conformation was changed by a series of local moves randomly chosen along the entire chain. We used a set of micromodifications which was successfully used previously for star-branched chain models on a simple cubic lattice: these were (i) one-bond chain end motion, (ii) two-bond chain end motion, (iii) two-bond kink motion, (iv) three-bond kink motion, (v) three-bond 90° crankshaft motion, (vi) branching point collective motion.[34] It was previously shown that this set of micromodifications was proper for studying confined star-branched chains.[40] A time unit can be defined based on these micromodifications: it consists of one attempt of all these motions per one polymer segment.[34]

The initial conformation of the model chain between a pair of walls at the given distance *d* was constructed in three different ways. The first type of starting conformation was a flat two-dimensional chain at the distance between the walls $d=3$ and subsequently then an equilibration run was carried out. The equilibration run consisted of $10^6-10^7$ time units. Then, the long production run consisting of $10^7-10^8$ time units was performed. In the next step the distance *d* was increased and the whole procedure of the equilibration and the production was repeated. The second type of starting conformation we used was a self-avoiding chain constructed at a given distance *d* and then equilibrated. The third type of starting conformation was obtained by the squeezing of the surfaces, i.e., starting from the free chain and then the surfaces were introduced at the shortest possible distance *d*. After the equilibration and the production run the procedure of squeezing took effect and the distance between surfaces *d* was gradually diminished. In all cases we carefully carried out the equilibration in order to obtain a conformation free of self-avoiding walk or two-dimensional chain features. It was found that the properties of the chain were independent of the type of starting conformation. For each chain's length the simulations were repeated 30 times—initial conformations were different for all runs. Additionally, a series of simulations were performed for star-branched polymers between two walls and with impenetrable obstacles. An obstacle had the shape of an extended rod along the *z* direction starting from one wall and ending on the other; this is shown in Fig. 1(b). The initial conformation of the chain with obstacles was constructed in two different ways. In the first method the obstacles were added randomly to the existing confined chain and the equilibration and production of Monte Carlo simulation runs were performed subsequently. In the second method the model chain was added as the self-avoiding walk to the existing surfaces and obstacles and then equilibrated and simulated. No differences were found in properties of chains obtained starting from both types of initial conformations.

## RESULTS AND DISCUSSION

Each star-branched polymer consisted of $f=3$ arms of equal length. The simulations were carried out for model polymers with the $n=17$, 34, 67, 134, 267 and 401 beads in an arm. This corresponds to the total number of beads in a chain $N=49$, 100, 199, 400, 799, and 1201, respectively. It was previously shown that this range of chain length was sufficient to study chain's scaling properties.[39,40] It was extended to $N=1201$ in order to study the mechanism of motion of longer chains. The distance between the walls was varied between $d=3$ (the shortest possible distance for which a polymer chain confined to a simple cubic lattice can move) up to $d=50$ (even the longest chains under consideration were not squeezed here[40]). In order to compare properties of chains independent of their length we had to perform simulations of polymer chains squeezed to the same degree. The comparable squeezing of the chain is achieved for the same values of reduced distance between the surfaces $d^*$ defined as

$$d^*=\frac{d}{2\langle S^2\rangle^{1/2}}, \tag{1}$$

where $\langle S^2\rangle$ is the mean-square radius of gyration of the entire star-branched chain. As the changes of polymer size and its mobility are mostly pronounced and interesting for distances $d^*<1$ we decided to carry out simulations for all chain length under consideration at $d^*=0.7$ (moderate squeezing) and 0.4 (highly squeezed chains). Due to the discreteness of our lattice model we were not able to achieve the exact values of $d^*=0.7$ and 0.4 in our simulations though we chose the parameters of simulations as close as

TABLE I. The confinement parameters.

| $N$ | $\langle S^2\rangle_0$ | $d$ ($d^*=0.4$) | $d$ ($d^*=0.7$) |
|---|---|---|---|
| 49 | 13.72 | 3 | 5 |
| 100 | 31.47 | 5 | 8 |
| 199 | 72.50 | 7 | 12 |
| 400 | 163.22 | 11 | 17 |
| 799 | 370.73 | 16 | 27 |
| 1201 | 619.45 | 20 | 35 |

possible to the above-given values. The exact values of $d^*$ used were presented in Table I. The number of obstacles used in the simulation was varied and they occupied from 0.01 to 0.10 of the entire space available in the Monte Carlo box.

The dynamic properties of star-branched chains were studied in detail in our previous work.[39,40] We showed that the self-diffusion coefficient did not change monotonically with the distance between the surfaces. The possible explanation of this fact was that the mechanism of motion changes when going from a three-dimensional to two-dimensional polymer chain. Here we wanted to add some comments on the scaling properties of the diffusion coefficient. It is clear that studying the dependence of the chain mobility on its length cannot be done for star-branched polymers within a slit with the same distance $d$. It was previously shown that some similarities of static and dynamic properties can be found for chains that were compressed to the same degree, i.e., for the same $d^*$. Therefore, for the sake of comparison we studied chains at the same distances $d^*$ instead of $d$. Self-diffusion coefficient was calculated as in our previous work, i.e., from the center-of-mass autocorrelation function.[40] As the motion of star-branched polymers in the $z$ direction is suppressed we were interested in the diffusion in the $xy$ plane only. In Fig. 2 we present the double logarithmic plot of the diffusion coefficient $D_{xy}$ as a function of the chain length $N$ for the reduced distance $d^*=0.4$ and 0.7. One can see that surprisingly there are no differences in dynamic behavior of chains for both distances. The mobility of chains for $d^*=0.4$ is only slightly lower when compared to the case of $d^*=0.7$. In order to determine the scaling exponent $\gamma$ in

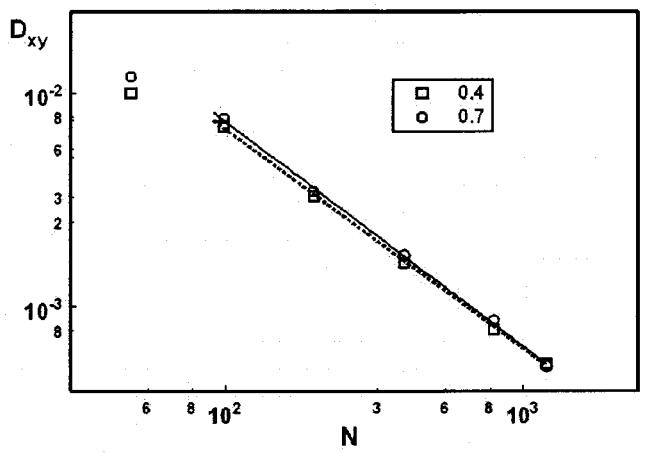


FIG. 2. The diffusion constant $D_{xy}$ as a function of chain length $N$ for reduced distances $d^*=0.7$ and 0.4 (see the inset).

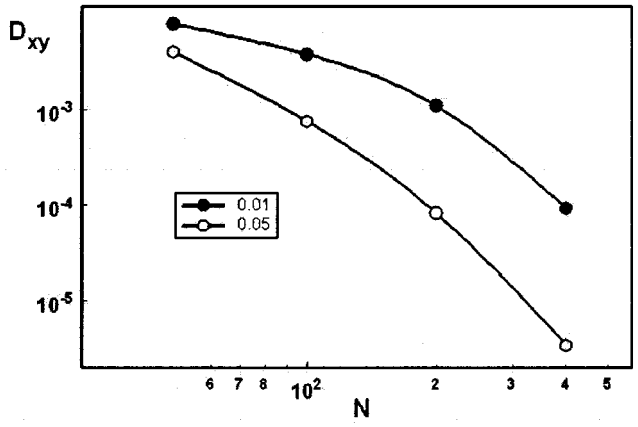


FIG. 3. The diffusion constant $D_{xy}$ as a function of chain length $N$ for different concentration of obstacles (see the inset).

the relation of $D_{xy}\sim N^{\gamma}$ we have taken into account longer chains which evidently obey this law ($N=49$ was neglected since it can bring some short chain lattice effects). The diffusion coefficient scales for both squeezing regimes as $N^{-1.03\pm0.01}$ and $N^{-1.05\pm0.02}$ for $d^*=0.4$ and 0.7, respectively.

Some additional information about the motion of confined star-branched chains can be deduced from the behavior of chain located between the surfaces with impenetrable obstacles. Figure 3 presents the diffusion coefficients of star-branched chains for the case of two different number of rods (obstacles): 100 and 500, which means that their concentration is 0.01 and 0.05, respectively. One can notice the most impressive feature of this plot, compared with the previous one, is that the curves are not linear. We have plotted the points for $N$ up to 400 only—the simulations for longer chains ($N=799$ and 1201) were impossible to perform due to the enormous amount of time needed for the translation required for determination of the stable diffusion coefficient. Taking into consideration the first two points ($N=49$ and 100 for concentration 0.01) one could determine the scaling relation as $N^{-1}$. However, this relation does not hold for the entire range of chain length—one can see that the plot is visibly curved. The same effect is seen for the obstacle concentration 0.05—the curvature of the plot depends in greater degree on chain length $N$. Theoretical consideration concerning star polymers in a matrix of very long chains also lead to the similar dependence of the diffusion coefficient on the chain length:

$$D\propto N^{-x}\exp\left(-\frac{\alpha N}{M_e}\right), \tag{2}$$

where $x$ is equal to 1, 2, or 3 depending on the particular theory and $M_e$ is the entanglement length.[41–43] This kind of star diffusion appeared when the ''arm retraction'' mechanism was involved and when this mechanism of motion was dominant. The experiments also indicated that this kind of tracer diffusion of star-branched chains was present.[44] Diffusion of our star-branched chains in a slit with rod-like obstacles had to have the same character too. Fitting our curves $D_{xy}(N)$ to Eq. (2) gave the best results of the parameter $x=-1$. The ration $\alpha/M_e$ was found to be 0.003 and 0.006 for

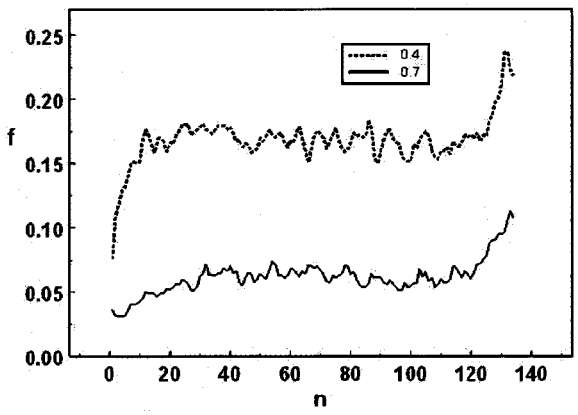


FIG. 4. The frequency of contacts polymer segment-surface $f$ as a function of the number of segments. The case of the chain with $N=400$ beads for $d^*=0.7$ and 0.4 (see the text for details).

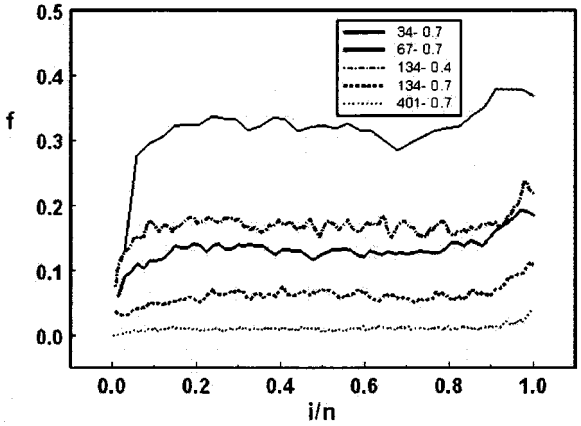


FIG. 5. The frequency of contacts $f$ as a function of the bead reduced number $i/n$. The chain lengths and the distances $d^*$ are given in the inset.

the concentration of obstacles 0.01 and 0.05, respectively. One also has to stress that for star-branched chains in a slit with no obstacles present this mechanism was rather not visible. Therefore, one can argue that for star-branched polymers in a slit formed by parallel impenetrable walls the arm retraction mechanism is nondominant.

The detailed analysis of the interactions of polymer chain with the confining surfaces was also done. The number of contacts between polymer segments and an impenetrable surface was a measure of the pressure the chains exerted on the wall. Moreover, it was also interesting to establish what was the frequency of these contacts for different parts of star-branched macromolecule. One can expect that the most frequent contacts would occur for these polymer segments which were not hidden in the middle of the polymer film. Figure 4 presents the mean frequency of polymer-surface contacts for star-branched chains consisting of $N=400$ beads for $d^*=0.7$ and 0.4. The frequency $f$ was calculated from the simulation trajectory as follows: for each trajectory snapshot the number of polymer–surface contacts were counted and then the mean values per one snapshot were calculated. The calculations of the frequency were performed for each polymer bead number separately. The numbering of a polymer bead started from the branching point (bead 1) and ended at arm's end (bead $n$) and was averaged for all arms. One can see from Fig. 4 that both curves were of similar shape but the frequency depended on the value of the distance $d^*$. This dependence was not linear, i.e., the decrease of $d^*$ by the factor 1.75 ($=0.7/0.4$) led to the increase of the frequency by the factor of 2.5. One can distinguish three regions in both curves: 1° the branching point vicinity (about 10 beads) in which the frequency was growing along the bead number but was visibly lower than for other parts of the chains, 2° the main part of the chain (for beads numbers between 12 and 120) for which a plateau was observed (some fluctuation were present), and 3° terminal region (the last 14 beads) where the frequency rose sharply with bead number. Similar behavior was found for the remaining chain lengths under consideration, which was presented in Fig. 5. In order to compare the properties of chains, which differed in length, we used the reduced bead numbering $i/n$ as abscissa, i.e., the bead number was divided by the arm length. One can observe that the contact's frequency strongly depended on the chain length: the shorter the chain the larger the frequency value. At first glance this behavior seemed unexpected but one has to remember that for longer chains the real distance between the plates $d$ had to be larger in order to maintain the constant value of $d^*$. Therefore, the edge of the Monte Carlo box along $z$ axis larger and most of the polymer beads can be found apart from the walls.

Following the idea of presentation of similarity of behavior of chains having different lengths we recalculated the frequencies $f$ as follows.[40] We have calculated the ratio

$$f_i^*=\frac{f_i\cdot n}{\Sigma_{i=1}^{n} f_i}, \tag{3}$$

where the frequency of contact $f$ was simply normalized to be comparable for all chain lengths under consideration. This quantity was presented as a function of the reduced bead number in Fig. 6. One can see that the curves had similar shape for all chain lengths. This shape was similar to that of the frequency of contacts (see Figs. 4 and 5). The plateau region was located for $i/n=0.1-0.9$. The region of the chain close to the branching point ($i/n<0.1$) was less exposed to

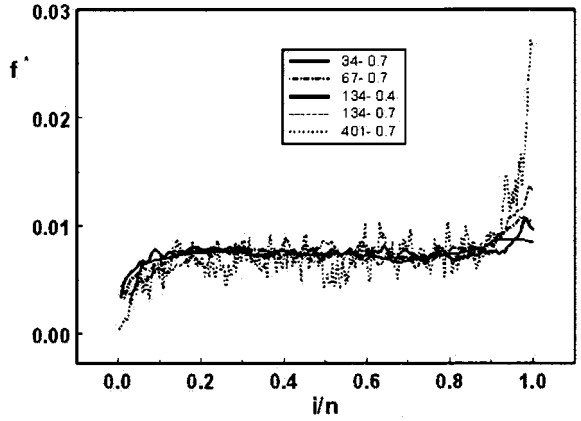


FIG. 6. The reduced frequency of contacts $f^*$ as a function of the bead reduced number $i/n$. The chain lengths and distances $d^*$ are given in the inset.

the surfaces than the other parts—on the other hand, the terminal part of the arms ($i/n>0.9$) exhibited very frequent contacts with surfaces than other parts of the chains. The fluctuations of the $f_i^*$ parameter increased with chain length. The successful construction of one common curve embedding the wide range of chain lengths and the distances between the surfaces revealed the internal structure of confined star-branched chains. An arm of the star could be divided into three sections that exhibit different properties.

The internal structure of star-branched chains between the walls can also be studied by the analysis of spatial distribution of polymer segments across the slit. Figures 7(a)–7(c) present density profiles for chain with $N=799$ beads along the $z$ axis. The three cases of the distance $d^*$ were presented in this figure: highly squeezed chain ($d^*=0.4$), moderately squeezed chain ($d^*=0.7$), and confined but almost not squeezed chain ($d^*=1.5$). In these figures we presented density profiles for the entire chain, the branching point and arm's ends. Following the idea of three different regions in the confined star-branched chain (see the above discussion on the frequency of contacts between polymer beads and the confining surfaces) we also plotted the density profiles for: first 10% of beads (called region I), inner beads (region II), and terminal 10% of beads (region III).

One can observe that all density profiles were symmetrical with a maximum located in the middle of the slit. However, there were noticeable differences in shape of distributions. All density profiles under consideration were Gaussian with the exception of curves for arm's ends and the region III which were rather parabolic. For the branching point and arm's ends profiles some fluctuations occurred, it was apparently caused by the worse statistics when compared to profiles for regions and all beads. The same reason caused distortion of the curves for the larger distances $d^*$. For all slit sizes under consideration the branching point almost never approaches the very surfaces while the majority of beads near the walls came from the arm's ends. For moderate and low squeezing of the chain the density profiles for the branching and arm's ends were almost identical with those for regions I and III, respectively. This observation was not valid for highly squeezed chains ($d^*=0.4$) where the probability of finding the branching point in the middle of the slit and arm's ends near the walls was considerably higher than that for regions I and III, respectively. The results concerning the density profile were in perfect agreement with the analysis of the number of contacts between polymer and both surfaces. Additionally, one can observe an interesting behavior of the density profiles which cross themselves at two points each at a distance roughly $d/3$ from the wall. In these points the effect of confinement of walls was compensated by the ''free'' polymer beads located in the middle of the slit. Therefore, we can distinguish three regions of the slit: two outer and one inner, each $d/3$ thick.

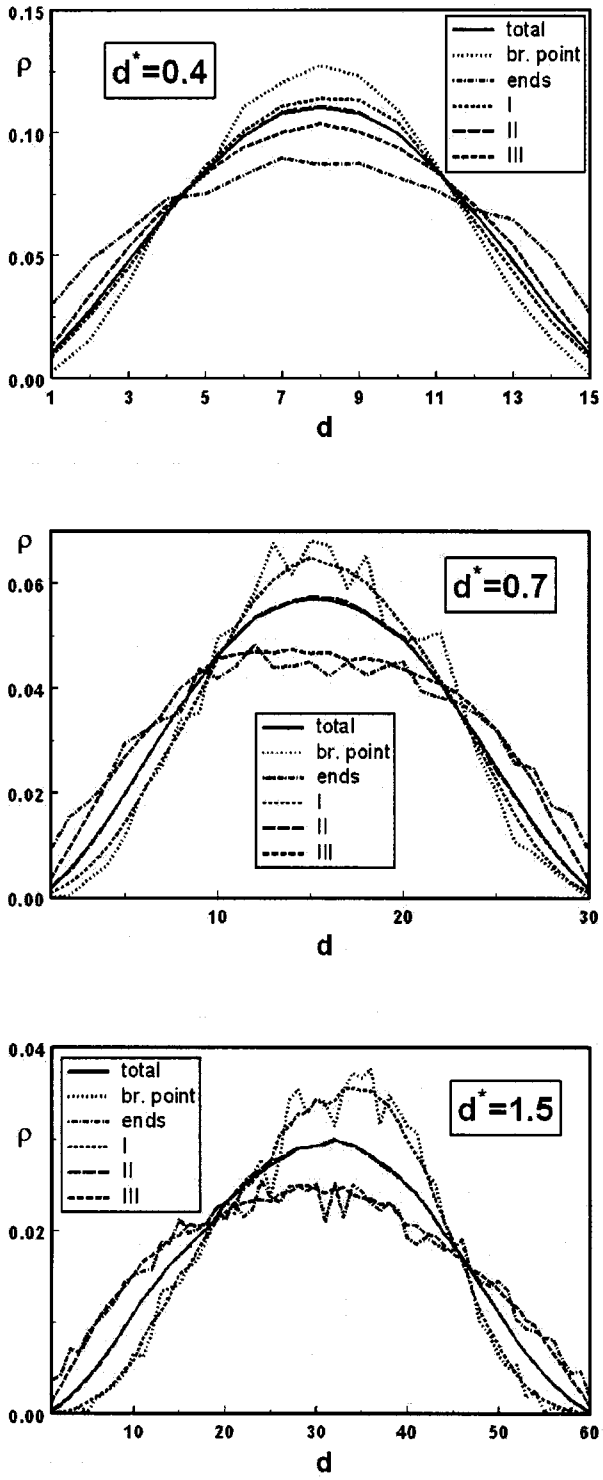


FIG. 7. Density profiles along the $z$ axis for all polymer segments, the branching point, arms' ends, and regions I–III (see the text for details). The case of the chain consisted of $N=799$ beads for $d^*=0.4$, 0.7, and 1.5, respectively.

## CONCLUSIONS

We studied simple models of star-branched polymers confined by two parallel impenetrable surfaces. A cubic lattice model of a macromolecule in good solvent conditions (athermal chain) was developed for this purpose. Monte Carlo simulations were carried out in order to determine the structure and dynamic properties of deformed chains. Some universal dynamic dependencies were expected, analogous to the static properties described in the previous work.[40]

The diffusion of chains was studied for different distances between surfaces. We determined the values of the

diffusion coefficient for $d^*=0.7$ and 0.4. Surprisingly, the substantial change in the compression of the chain (from $d^*=0.7$ to 0.4) reduced the mobility of the system in small degree. Also the scaling of the diffusion coefficient was found to be almost independent on the $d^*$ and thus on the compression of the chain: $D_{xy}\sim N^{-1}$. This scaling was identical to that for unconfined chains.[34,36] The introduction of impenetrable rod-like obstacles into the slit apparently did not change the mobility of chain dramatically but the dependence of the diffusion coefficient on the chain length was changed. The diffusion of star-branched chain in a slit with obstacles indicated that the ''arm-retraction'' mechanism was probably present there.

A detailed analysis of contacts formed by polymer segments with the confining surfaces was carried out. It was found that the number of contacts strongly depended on its location along the star arm's contour, i.e., on its numbering. For the middle part of an arm containing 80% of arm's beads the number of contacts was almost constant. On the other hand, for both terminal 10% of the arm's beads contacts strongly depended on the position of the given bead in the chain. The vicinity of the branching point was strongly screened by outer beads whilst the beads close to the arm ends expressed the tendency to stay near the confining surfaces.

Polymer density profiles across the slit were analyzed for the entire chain and for its fragments. It was found that the total density profile was Gaussian for all chains under consideration and for all distances between the walls. The profiles for branching point and the part of an arm near the branching point showed that they almost never contacted the wall whilst the arm's ends and the terminal parts of arms can be often found in the vicinity of the wall.

The above considerations enable one to state that in the case of the star-branched chains the properties of the system are the function of its architecture. The inner part of the star-branched chain with a high concentration of the polymer beads usually called ''core'' is mainly located near the middle of the slit.[35] The knowledge of the structure of the polymer system in confined space is essential for understanding the mechanism of motion of these objects.

[1] R. Eisenriegler, *Polymers Near Surfaces* (World Scientific, Singapore, 1993).
[2] S. Granick, Science **253**, 1374 (1991).
[3] J. H. van Vliet and G. ten Brinke, J. Chem. Phys. **93**, 1436 (1990).
[4] E. Giesen and I. Szleifer, J. Chem. Phys. **102**, 9069 (1995).
[5] A. Milchev and K. Binder, J. Phys. II **6**, 21 (1996).
[6] E. Cordeiro, M. Molisana, and D. Thirumalai, J. Phys. II **7**, 433 (1997).
[7] B. Erman and L. Monnerie, Macromolecules **30**, 5075 (1997).
[8] N. Semenov, J. F. Joanny, A. Johner, and J. Bonet-Avalos, Macromolecules **30**, 1479 (1997).
[9] A. Milchev and K. Binder, Eur. Phys. J. B **3**, 477 (1998).
[10] P. Cifra and T. Bleha, Macromol. Theory Simul. **8**, 603 (1999).
[11] V. Kuznetsov and A. C. Balazs, J. Chem. Phys. **113**, 2479 (2000).
[12] S. Jorge and A. Rey, J. Chem. Phys. **106**, 5720 (1997).
[13] Y. Yoshida and Y. Hiwatari, Mol. Simul. **22**, 91 (1999).
[14] T. W. Burkhardt and I. Guim, Phys. Rev. E **59**, 5833 (1999).
[15] P. Sotta, A. Lesne, and J. M. Victor, J. Chem. Phys. **113**, 6966 (2000).
[16] D. Viduna, Z. Limpouchova, and K. Prochazka, J. Chem. Phys. **115**, 7309 (2001).
[17] G. ten Brinke, D. Ausserre, and G. Hadziioannou, J. Chem. Phys. **89**, 4374 (1988).
[18] S. K. Kumar, M. Vacatello, and D. Y. Yoon, J. Chem. Phys. **89**, 5206 (1988).
[19] T. Pakula, J. Chem. Phys. **95**, 4685 (1991).
[20] T. Pakula and E. B. Zhulina, J. Chem. Phys. **95**, 4691 (1991).
[21] H.-W. Hu and S. Granick, Science **258**, 1339 (1992).
[22] E. B. Zhulina and T. Pakula, Macromolecules **25**, 754 (1992).
[23] R. G. Winkler, T. Matsuda, and D. Y. Yoon, J. Chem. Phys. **98**, 729 (1993).
[24] A. Yethiraj, J. Chem. Phys. **101**, 2489 (1994).
[25] J. Baschnagel and K. Binder, J. Phys. I France **6**, 1271 (1996).
[26] A. N. Semenov, A. V. Subotin, G. Hadziioannou, G. ten Brinke, E. Manias, and M. Doi, Macromol. Symp. **121**, 175 (1997).
[27] R. B. Pandey, A. Milchev, and K. Binder, Macromolecules **30**, 1194 (1997).
[28] J.-U. Sommer, A. Hoffmann, and A. Blumen, J. Chem. Phys. **111**, 3728 (1999).
[29] T. Aoyagi, J. Takimoto, and M. Doi, J. Chem. Phys. **115**, 552 (2001).
[30] E. Manias and V. Kuppa, Eur. Phys. J. E **8**, 193 (2002).
[31] A. Milchev, Eur. Phys. J. E **8**, 531 (2002).
[32] G. S. Grest, L. J. Fetters, J. S. Huang, and D. Richter, Adv. Chem. Phys. **94**, 67 (1996).
[33] J. J. Freire, Adv. Polym. Sci. **143**, 35 (1999).
[34] A. Sikorski, Macromol. Theory Simul. **2**, 309 (1993).
[35] A. Sikorski, A. Koliński, and J. Skolnick, Macromol. Theory Simul. **3**, 715 (1994).
[36] P. Romiszowski and A. Sikorski, J. Chem. Phys. **104**, 8703 (1996).
[37] A. Sikorski and P. Romiszowski, J. Chem. Phys. **109**, 2912 (1998).
[38] A. Sikorski and P. Romiszowski, Macromol. Theory Simul. **8**, 109 (1999).
[39] P. Romiszowski and A. Sikorski, Macromol. Symp. **171**, 63 (2001).
[40] P. Romiszowski and A. Sikorski, J. Chem. Phys. **116**, 1731 (2002).
[41] P. G. de Gennes, J. Phys. (Paris) **36**, 1199 (1975).
[42] J. Klein, Macromolecules **19**, 105 (1986).
[43] C. R. Bartels, B. Crist, Jr., L. J. Fetters, and W. W. Graessley, Macromolecules **19**, 785 (1986).
[44] J. Klein, D. Fletcher, and L. J. Fetters, Nature (London) **304**, 526 (1893).